EFFECT OF MUSCLE CONTRACTION ON KNEE LOADING FOR A STANDING PEDESTRIAN IN LATERAL IMPACTS

Anurag Soni
Anoop Chawla
Sudipto Mukherjee
Department of Mechanical Engineering
Indian Institute of Technology Delhi, India
Paper Number 07-0458

ABSTRACT

Knee injury thresholds are based on cadaver experiments and do not take into account active muscle contributions. Preliminary studies have indicated that muscle forces reduce injury risk in knee ligaments [Soni et al, 2006]. In this paper we study the effect of active muscle forces on knee bending angle and shear displacements for a free standing pedestrian in lateral impacts using PAM-CRASH^{TM}.

A passive FE model has been developed and validated for tests reported in Kajzer et al. (1997, 1999) and Kerrigen et al. (2003). An **A**ctive **L**ower **E**xtremity **M**odel for **S**afety (**A-LEMS**) has then been developed by including forty seven lower extremity muscles. A-LEMS has then been used to simulate below knee and ankle impacts in free standing pedestrians with activated and deactivated muscles.

The FE model shows good correlation with both Kajzer's and Kerrigan's tests results. On incorporating active muscles, it is observed that ligament strains decrease, even though the Von Mises stresses in the bones do not show a significant difference. Knee bending angle and shear displacement curves also show lower peaks with active muscles.

We conclude that muscle activation reduces ligament strains, as well as knee bending angles and shear displacements. It suggests that knee injury thresholds can be different from those formulated on the basis of cadaver studies. Therefore muscle effects should be taken into account in deciding vehicle safety standards and injury predictions in pedestrian crashes.

In this study we have assumed a straight line of action for muscles. This can lead to errors for muscles which do not work along a straight line. Tendons should also been included for more accurate muscle modeling. Currently, the study is also limited to the standing posture only and other postures are being investigated.

The current study investigates the effect of active muscle forces on the knee injury thresholds for a standing pedestrian.

INTRODUCTION

The issue of pedestrian safety has been a matter of concern for public health practitioners and vehicle designers (Ashton et al., 1977). Pedestrians represent 65% of the 1.17 million people killed annually in road accidents worldwide (World Bank, 2001). Epidemiological studies on pedestrian victims have indicated that together with the head, the lower extremities are the most frequently

injured body region (Chidester et al., 2001; Mizuno, 2003). The 2003 summary report of International Harmonized Research Activities (IHRA) Pedestrian Safety Working Group activity (Mizuno, 2003) has showed that 1,605 pedestrian victims in Australia, Germany, Japan and USA, sustained a total of 3,305 AIS 2+ injuries, out of which almost one third (32.6%) were to the lower extremity. The injuries to lower extremities in car crashes mainly include bone fractures and avulsion or stretching in knee ligaments (Mizuno, 2005). To mitigate the incidences and extent of lower limb injuries, it is essential to understand the mechanism of these injuries, and both experimental as well as numerical methods have been widely used for this purpose.

For ethical reasons, volunteer experiments cannot be performed in the higher injury severity range similar to those in pedestrian-car crashes. Therefore, the loading environment in pedestrian-car collisions has been characterized by experiments using Post Mortem Human Specimen (PMHS) (Bunketorp et al., 1981; 1983; Aldman et al., 1985; Kajzer et al., 1990; 1993; 1997; 1999; Ramet et al., 1995; Bhalla et al., 2003; 2005; Kerrigan et al., 2003; Bose et al., 2004; Ivarsson et al., 2004; 2005). As cadavers have been used in these experiments, these studies could not consider the effect of live muscle actions such as involuntary muscle reflexes, pre-impact voluntary muscle bracing etc. Mechanical legforms (the EEVC legform by TRL; FlexPLI (Konosu et al., 2005); Polar II pedestrian dummy by Honda R&D; frangible legform by Dunmore et al., 2005) have also been developed on the basis of these tests, and as a result do not account for muscle forces.

Finite element (FE) studies offer an alternate method of studying these effects. However, none of the earlier versions of validated FE models of pedestrian lower extremities (Schuster et al., 2000; Maeno et al., 2001; Takahashi et al., 2001; 2003; Matsui et al., 2001; Nagasaka et al., 2003; Chawla et al., 2004) inculde the effects of muscle actions.

Recently, Soni et al. (2006) has developed a pedestrain lower limb FE model including 40 lower extremity muscles. This model has been used to investigate the effects of pre-impact muscular contraction on knee ligament forces in lateral impacts for free standing posture of a pedestrian. Results of this preliminary investigation indicate that muscle activation decreases the probability of failure in knee ligaments.

Recently, Soni et al. (2006) has developed a pedestrain lower limb FE model including 40 lower extremity muscles. This model has been used to investigate the effects of pre-impact muscular contraction on knee ligament forces in lateral impacts for free standing posture of a pedestrian. Results of this preliminary investigation indicate that muscle activation decreases the probability of failure in knee ligaments. However, the base model used in this study has shortcomings in both geometry and material representation such as lack of bio-fidelity of base model, requirement of knee capsule, improvements needed in knee ligaments geometry, finite element selection and their material properties as reported in Chawla et al. (2004).

In the present study, we have aimed to improve our preliminary model reported in Soni et al. (2006) and then to use the improved model to study the effects of muscle contraction. Therefore, as a first step it has been decided to improve the passive response of knee joint in our basic lower extremity model developed by Chawla et al. (2004). For this purpose, geometry and material properties of knee ligaments has been modified. Knee capsule has been included as suggested by Chawla et al. (2004). Material properties of cortical as well as spongy part of bones are also modified. Then the

modified lower extremity model has been validated against the test results of Kajzer et al. (1997, 1999) and Kerrigan et al. (2003).

In the next step, Active Lower Extremity Model for pedestrain Safety (A-LEMS) has been developed. Therefore, 42 lower extremity muscles represented as 1-D bar elements are added in the validated FE model. Hill material model has been assigned to each lower extremity muscle to capture muscle contraction. A-LEMS is then used to model the standing posture of a cadaver, an aware and an unaware pedestrian. Knee bending moment, lateral shear force, knee bending angle, lateral shear displacement and strains in knee ligaments have then been compared for all three pre-impact pedestrian configurations.

FE MODEL DESCRIPTION

For the current research work, lower extremity FE model developed by Chawla et al. (2004) has been adopted as a base model. Due to the shortcomings existed in base model we have modified it to improve its response for passive loading cases.

Model Geometry

The modified model used in the present work includes the cortical and the spongy parts of the femur, tibia, fibula, and the patella. The cortical part of the bones is modeled by shell elements while the spongy part is modeled by solid elements. Apart from these, passive muscle and skin are also modeled using solid elements and membrane elements respectively. Knee ligaments, anterior cruciate ligament (ACL), posterior cruciate ligament (PCL), and lateral collateral ligament (LCL), have been modeled using solid elements. However, due to the smaller thickness in comparison to width, medial collateral ligament (MCL) has been modeled using the shell elements. To model knee ligaments, details regarding their cross-sectional areas have been taken from Takahashi et al. (2000), however, their orientations and the attachment locations on the bones have been kept similar as in our base model. Articular capsule i.e. “Knee capsule”, which encloses the knee joint and maintains joint integrity, has been included in this model. Therefore, a surface mesh enclosing the tibia plateau and the distal femur condyles has been constructed using the shell elements in HyperMeshTM.

Material Properties

Appropriate material models have been selected from the available material library of PAM-CRASH^{TM} for each part of the FE model to capture their mechanical behavior in simulation.

Spongy and the cortical parts of the bones (femur, tibia and fibula) are assumed to be isotropic elastic-plastic materials. Therefore, material models, Material # 16, and Material # 105 is used for spongy and cortical parts of the bones respectively. Takahashi et al. (2000) have done an extensive survey to determine the mechanical properties of the cortical and spongy parts of the femur and tibia. Therefore, bones mechanical properties reported in their study (listed in
Table 1) are used in our model.

Knee ligaments are assumed to behave as isotropic elastic-plastic material. Therefore, elastic-plastic material model, Material # 16 (for solid elements) is assigned to ACL, PCL and LCL, whereas Material # 105 (for shell elements) is used for MCL. Five mechanical parameters such as elastic modulus, yield stress, yield strain, ultimate stress and ultimate strain are required to charaterize the eastic-plastic behviour of knee ligaments. Values of these parameters for ACL PCL and LCL have been estimated from an experimental study conducted by Butler et al. (1986) and the similar values have been assumed for MCL. Table 2 lists the material properties assigned to knee ligaments in the FE model. Element elimination approach has been used to simulate the failure in knee ligaments. Ultimate strain value is used as the failure

threshold to initiate the element elimination process. In this process, stiffness of the element decreases to zero over 100 time steps once it is initiated. However, nodes of the eliminated elements are retained in the simulation to maintain their mass, kinetic energy, and contact properties.

Material properties of knee capsule is not available in literature, therefore material properties assigned to skin is used as an initial estimation. For the remaining lower extremity structures, material properties defined in the base model has been retained.

Table 1.

Mechanical properties of bone taken from Takahashi et al. 2001

Material Name	Density (kg/m3)	Elastic Modulus (MPa)	Yield Stress (MPa)	Yield Strain (%)	Poisson's Ratio	Ultimate Stress (MPa)	Ultimate Strain (%)
Femur Cortical	2000	14317	114.1	0.8	0.315	123.3	2.0
Tibia Cortical	2000	20033	129.0	0.63	0.315	138.1	1.5
Femur Spongy	1000	295	3.7	1.25	0.315	3.7	13.4
Tibia Spongy	1000	295	3.7	1.25	0.315	3.7	13.4

Table 2.

Mechanical properties of knee ligaments

Knee Ligaments	Density (kg/m3)	Elastic Modulus (MPa)	Yield Stress (MPa)	Yield Strain (%)	Poisson's Ratio	Ultimate Stress (MPa)	Ultimate Strain (%)
ACL, PCL, LCL, MCL	1100	345	29.8	8.64	0.22	36.4	15

FE MODEL VALIDATION FOR PASSIVE LOADING CASES

Before incorporating the muscles in the FE model it is essential to investigate the validity of the knee joint in the lower extremity model. Therefore, FE model has been validated against the PMHS test results reported by Kajzer et al. (1997, 1999) and Kerrigan et al. (2003).

Validation for Kajzer's Tests

Kajzer et al. (1997, 1999) conducted impact experiments on PMHS to load cadaver knee joints in shear and bending. These tests are intended to recreate the impact conditions usually occur in case of vehicle-pedestrian collisions. Loading and the boundary conditions used in these experiments are shown in

Figure 1.

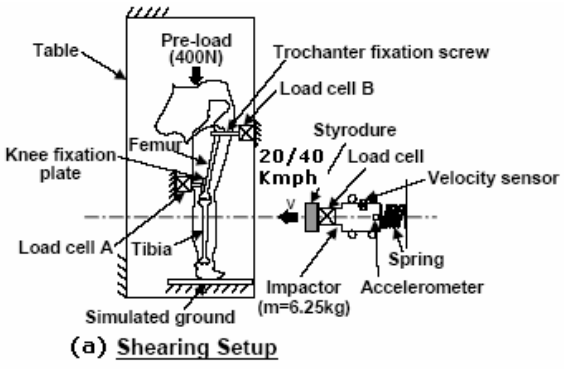

(a) Shearing Setup

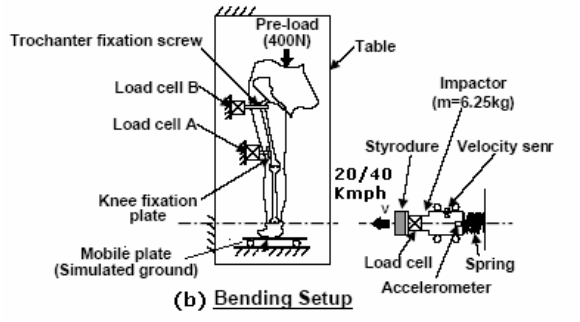

Figure 1. Kajzer's tests setup

In these tests, PMHS is laid supine on its back on the table. A plate perpendicular to the table, representing the ground, is used to support the foot of the cadaver. In case of knee shearing, foot support plate is kept fixed, whereas, in knee bending rollers are placed between the foot and the support plate to prevent the development of friction force. Preload of 400 N, corresponding to half of the body weight of a cadaver, is applied to the torso. To concentrate the impact load at the knee joint, femur is screwed at two locations. A foam covered impactor of 6.25 kg mass is propelled in lateral direction at a speed of 20 kmph and 40 kmph to impact at just below knee (shear tests) and at ankle locations (bending tests) of the leg. Wittek et al. (2000) has conducted a detailed analysis of these experiments to obtain the PMHS response corridors. These corridors have been used to validate the kinematics of knee joint in our FE model.

Experimental conditions used in Kajzer's tests have been reproduced in FE simulations. Figure 2 shows the setups used in the simulation.

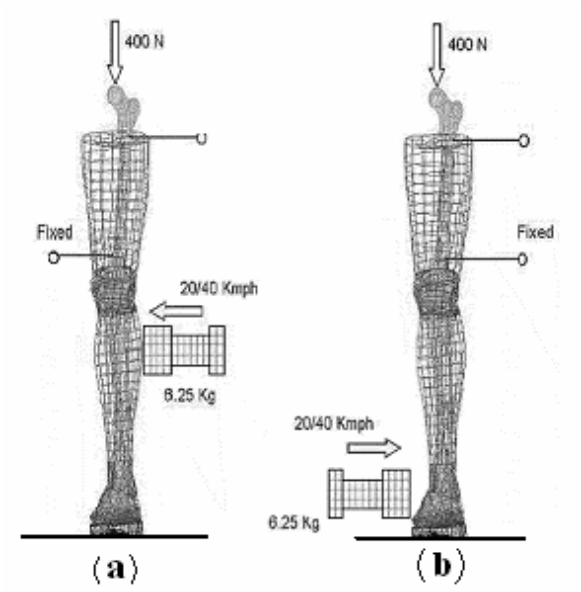

Figure 2. Simulation setup for Kajzer's tests

A rigid support plate, representing the ground in the tests, is modeled under the foot using shell elements. Coefficient of friction between the foot and support plate is kept low (0.01) in knee bending simulations to consider the effects of rollers used in bending tests. However, a relatively high value of coefficient of friction (0.3) is used in knee shearing simulations. Nodes corresponding to the upper and lower locations on the femur cortical bone are fully restrained to represent the constraints on femur in experiments. A vertical load of 400 N is applied at the top of the femur to represent the half body weight. A foam covered rigid impactor of 6.25 kg has been modeled. An initial velocity of 20 and 40 kmph has been assigned to center of gravity of the rigid impactor to propel it towards the leg. Gravity imposed acceleration field has also been modeled in all the simulations.

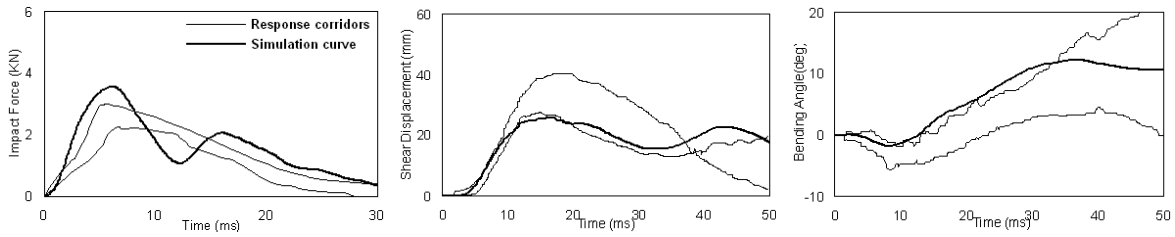

Figure 3. Comparison between PMHS response corridors and simulated impact force, shear displacement and bending angle for knee shearing at 20 Kmph

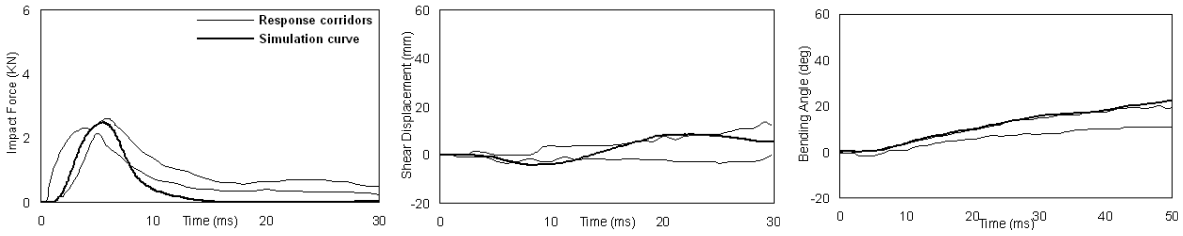

Figure 4. Comparison between PMHS response corridors and simulated impact force, shear displacement and bending angle for knee bending at 20 Kmph.

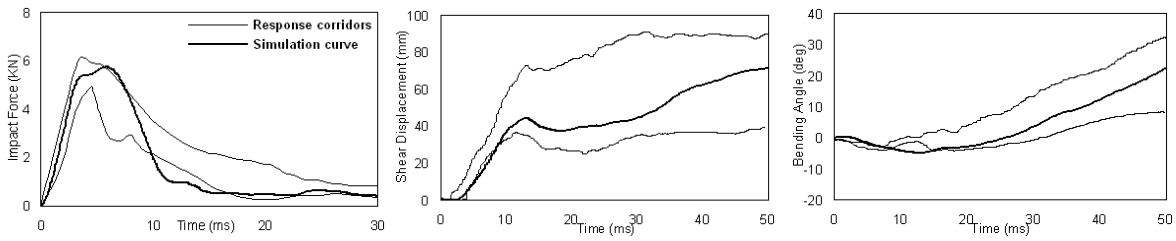

Figure 5. Comparison between PMHS response corridors and simulated impact force, shear displacement and bending angle for knee shearing at 40 Kmph.

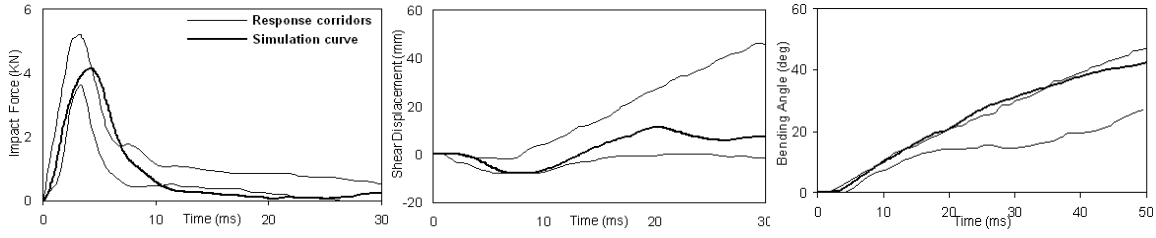

Figure 6. Comparison between PMHS response corridors and simulated impact force, shear displacement and bending angle for knee bending at 40 Kmph.

Table 3.

Injury description in shearing and bending setup at 20 Kmph for both experiment and simulation

Shearing

	Knee Ligaments			
	ACL	PCL	MCL	LCL
Simulation	☆			
Test # 21S	●			
Test # 24S				
Test # 25S				
Test # 29S	●			

Bending

	Knee Ligaments			
	ACL	PCL	MCL	LCL
Simulation			☆	
Test # 23B				
Test # 26B				
Test # 27B			●	
Test # 30B			●	

☆- Failure in simulation

● - Failure in experiment

Table 4.

Injury description in shearing and bending setup at 40 Kmph for both experiment and simulation

Shearing

	Knee Ligaments			
	ACL	PCL	MCL	LCL
Simulation	☆	☆	☆	
Test # 1S				
Test # 8S	●			
Test # 16S	●			

Bending

	Knee Ligaments			
	ACL	PCL	MCL	LCL
Simulation	☆	☆	☆	
Test # 3B		●	●	
Test # 6B	●	●	●	
Test # 19B	●		●	

Figures 3-6 shows the comparison between PMHS response corridors and simulated impact force, shear displacement and bending angle for both knee shear and bending tests at 20 Kmph and 40 kmph speed. Results indicate that the simulated response of the knee joint in FE model lies within the experimental corridors. Table 3 and Table 4 summarize the comparison of knee ligament failures observed in simulations and the failure reported in the corresponding PMHS tests. The simulated failures match with the experimental failures. Thus, the lower extremity FE model validates for Kajzer's loading and boundary conditions and is capable of reproducing the failures in knee ligaments correctly.

Validation for Kerrigan's Tests

Knee joint FE model is validated against the displacement controlled dynamic four point bending and shearing tests conducted on isolated

cadaver knees in Kerrigan et al. (2003).

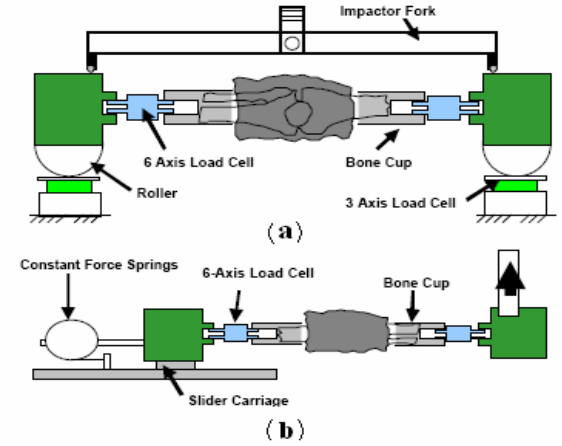

Figure 7 shows the schematics of both the experiments.

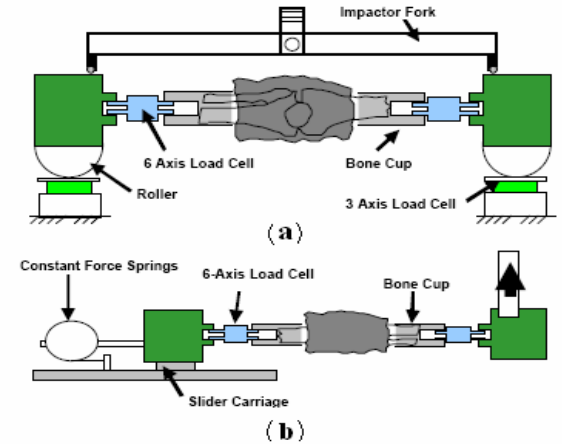

Figure 7. Schematic diagrams of dynamic (a) four point bending tests and (b) shearing tests (Reproduced from Kerrigan et al. 2003).

In four point bending tests, the end boxes are mounted on the metal rollers which are then placed on the supports. These rollers are set free to rotate in the coronal plane as well as to translate in the superoinferior direction. A twin pronged impactor is displaced with an average velocity of 0.6 m/s. Both the prongs of the impactor fork contact the inside edges of the metal end boxes and therefore push it dynamically in the lateromedial direction. As the loading locations are symmetric and are within the supporting span, this configuration has characterized the isolated cadaver knee joints in pure bending.

In knee shearing tests, the end box on the proximal side (femur side) is fixed to a slider carriage. Therefore it is only allowed to translate in the superoinferior direction. A constant force of 700 N is applied in the axial direction of the long bone. The end box on the other side (tibia side) is rigidly attached to the actuator of the displacement controlled servo-hydraulic test machine. Actuator is displaced in the lateromedial with a constant velocity of approximately 1.1 m/s. The configuration used in this test has characterized the isolated cadaver knee joints in pure shearing.

Recently, Bhalla et al. (2005b) have scaled the Kerrigan's test results (i.e. bending moment v/s bending angle and shear force v/s shear displacement plots) to the anthropometry of a 50th percentile male in order to account for the varying anthropometry of subjects tested. These scaled results have been used to validate our FE model.

Test conditions reported in Kerrigan et al. (2003) have been reproduced in FE simulations. Figure 8 shows schematic diagrams of the simulation setups representing the bending and shearing tests.

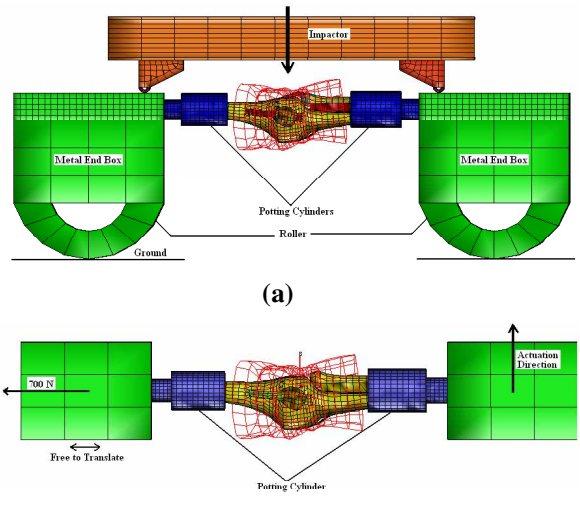

Figure 8. Simulation setup for (a) four point knee bending (b) dynamic knee shear tests performed in Kerrigan et al. (2003)

To model the test conditions, FE mesh of the knee joint including distal part of femur, proximal parts of tibia-fibula complex, knee ligaments, joint capsule, meniscus and the flesh around the knee has been segregated from our full lower extremity model. Apart from this, all the parts of the test apparatus such as potting cylinders, load cells, end boxes, metal rollers, and the twin pronged impactor are modeled using solid elements in HyperMesh™ and are defined to be rigid in simulations. In simulations, appropriate contacts are modeled between the interacting bodies

For bending simulations, center of gravity of impactor has been displaced in lateral-medial direction with a constant velocity of 0.6 m/s. The end boxes are allowed to rotate in coronal plane as well as to translate in the superioinferior direction. Two nodes at each potting cylinders have been selected to capture nodal time history plots in simulation. Relative movements of selected nodes are then used to calculate knee bending angle. A transverse plane at the center of knee joint has been defined in simulation to calculate the knee bending moment. The bending stiffness of knee model has been then compared with the bending stiffness of the cadaver knee obtained through the experiment.

In shearing simulations, the end box on the proximal side (femur side) is constrained to translate only in superoinferior direction whereas; the end box at distal side (tibia side) is displaced with a constant velocity of 1.1 m/s in lateromedial direction. A constant axial compressive force of 700 N is applied to the proximal end box. Node assigned to center of gravity of the distal end box is used to calculate the knee lateral-medial shear displacement in simulation. A transverse plane at knee center is defined to calculate the knee shear force. Shear stiffness of the knee joint model is calculated and compared with the shear stiffness of the cadaver knee obtained through the experiments. In both bending and shearing simulations, failure occurring in knee ligaments has been compared with the ligament injuries reported in the respective experiments to assess the capability of our model in predicting the injury patterns.

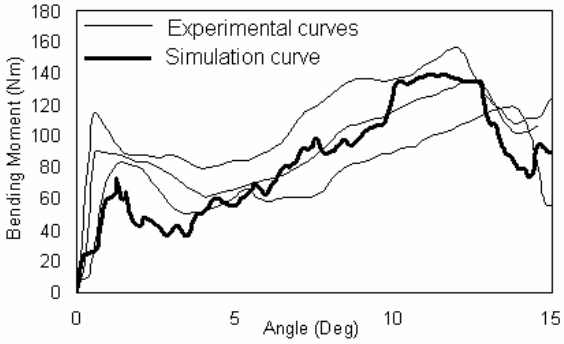

Figure 9. Comparison between simulated knee joint bending stiffness with that of obtained in cadaver experiments

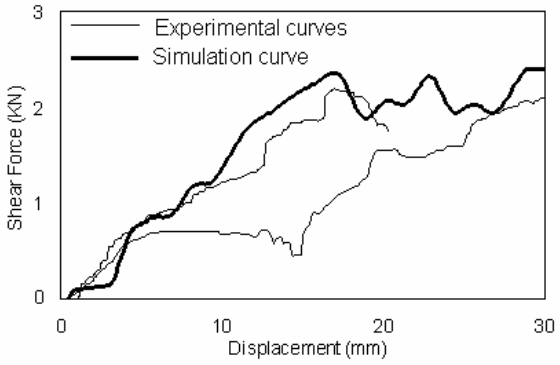

Figure 10. Comparison between simulated knee joint shear stiffness with that of obtained in cadaver experiments

Table 5.

Injury description in four point knee bending test for both experiment and simulation

	Knee Ligaments

	ACL	PCL	MCL	LCL
Simulation			☆	
Test # 1			●	
Test # 2			●	
Test # 3			●	

Table 6.

Injury description in dynamic knee shear test for both experiment and simulation

	Knee Ligaments			
	ACL	PCL	MCL	LCL
Simulation	☆			
Test # 1	●			
Test # 2	●			
Test # 3	●			

Figure 9 shows the comparison between the simulated and the experimental variation of knee bending moment with bending angle. Results suggest that bending stiffness of the FE knee joint is similar to that of tested cadaver knees. Table 5 gives the description of failure occurred in simulation and experiments. It is observed that MCL is the only ligament which fails in both simulations and experiments.

Similarly, Figures 10 compares the simulated and the experimental variation of knee shear force with shear displacement. Results indicate that shear stiffness of the FE knee joint is similar to that of tested cadaver knees. It is observed that ACL is the only ligament which fails in both simulations and experiments (see Table 6).

Knee joint of lower extremity FE model has been vaidated against the different sets of loading and boundary conditions reported in Kajzer et al. (1997, 1999) and Kerrigan et al. (2005). Validation results suggest that the model vaildates for all the test conditions and is also capable of reproducing the failure in knee ligaments correctly.

DEVELOPMENT OF A-LEMS

Validation of our FE model ensures its suitability for further study. Therefore, to study the effects of muscle contraction as the next course of action, 42 lower extremity muscles have been added in the validated FE model. This model has been then named as Active Lower Extremity Model for pedestrian Safety (A-LEMS).

Figure 11 shows the 42 lower extremity muscles modeled in A-LEMS.

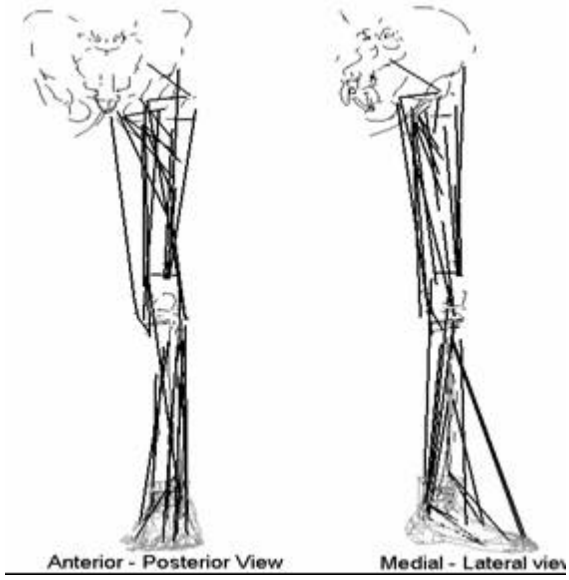

Figure 11. Anterior-posterior and Medial-Lateral views showing 42 lower extremity muscles modeled as bar elements for a standing posture. Origin and insertion location of these muscles are defined according to White et al. (1989).

Muscle Modeling

All the muscles modeled in this study is considered to exhibit straight line of action, therefore individual muscle is modeled using 1-D bar elements. Hill material model is defined for each muscle to capture its behavior in simulations.

Detailed description of muscle modeling has been provided in our previous study Soni et al. (2006). Similar approach has been followed to model the muscle to conduct the present work.

Hill Model Parameters

Muscle parameters, such as optimal muscle length (L_{opt}), maximum isometric force ($F_{\max}$), maximum contraction/ elongation velocity ($V_{\max}$), pennation angle (α), and an initial value of activation level (N_a), are required to define the Hill type muscle bar element.

Data for maximum isometric force ($F_{\max}$) and pennation angle (α) for each muscle are taken from Yamaguchi et al. (1990). Optimal muscle length (L_{opt}), at which a muscle produces maximum forces, has been adopted from Delp et al. (1980).

Maximum contraction velocity ($V_{\max}$) of a muscle depends upon the fraction of slow and fast type of fibers in it. Therefore, a muscle containing more fraction of fast type of fibers will be able to contract faster. Based on the material data available on mammalian muscles, Winters et al. (1985) has formulated an empirical relation (Equation 1) between the maximum contraction velocity of a muscle and the fraction of fast type of fibers it contains.

$$V_{\max} = 2 * Lofib(s^{-1}) + 8 * Lofib(s^{-1}) * C_{fast} \quad (1).$$

Where, L_{ofib} represents the muscle rest fiber length and C_{fast} fraction of fast fibers in a muscle.

Equation (1) has been used to calculate the maximum contraction velocity for each muscle and the data required for L_{ofib} and C_{fast} has been taken from Yamaguchi et al. (1990).

An activation level (N_a) represents the state of a muscle. It is defined as the ratio of a current force to the maximum force that can be exerted by a muscle. Thus it is a dimensionless quantity ranges from a minimum value of 0.005 to maximum value of 1. Activation value of 0.005 represents a muscle at rest whereas maximum value (i.e.1) represents maximum activation in a muscle, such as that for a maximum voluntary contraction (Winters et al., 1988).

Data used to define the Hill muscle card of each muscle in A-LEMS has been listed in Appendix A.

SIMULATIONS FOR STANDING POSTURE

Effect of muscle activation in a free standing posture of a pedestrian has been studied next. Therefore, in these simulations A-LEMS has been configured as freely standing on rigid ground plate in a gravity field. To represent the friction between road and shoe correctly, a value of 1.0 has been defined as a coefficient of friction between the shoe and ground in simulations. A 250 N load corresponding to half the body weight of a 50th percentile male minus weight of A-LEMS has been applied at the top of the femur.

Then a foam covered rigid impactor of 20 kg mass has been propelled in lateral direction at a speed of 25 kmph to impact A-LEMS at two locations i.e. below-knee and at-ankle. Bhalla et al. (2005a) has reported that for a 50th percentile male, centerline of the car bumper hits the lower leg 45 mm below the tibia plateau. Therefore to reproduce the real world vehicle-pedestrian impact conditions for below knee impact, we have also positioned the impactor such that the center line of impact should be 45 mm below the of tibia plateau. Whereas, for ankle impact, impactor is positioned such that it should hit the ankle at its center.

Figure 12 shows the simulation setups for both below-knee and at-ankle impact.

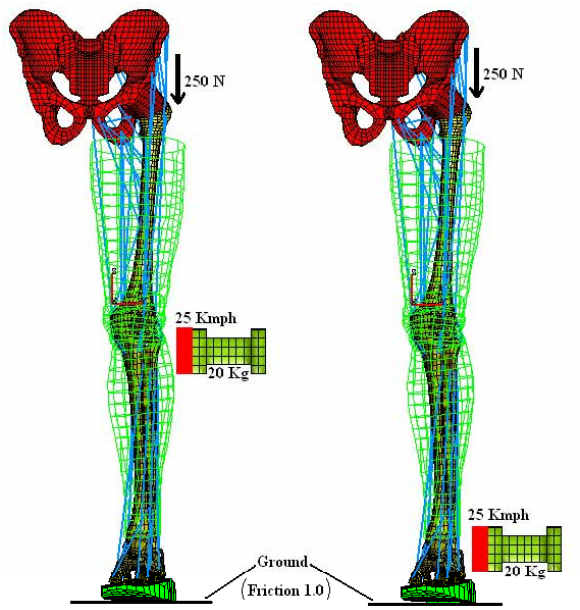

Figure 12. Simulation setups for below knee and ankle impact.

Three sets of simulations (S1, S2, and S3) have been performed for each impact location. In each set of simulation, muscles in A-LEMS have been modeled such that it represents a different pre-impact configuration of a pedestrian occur in real world.

In S1, a quiet standing pedestrian who is unaware of an accident has been simulated. Therefore, to model A-LEMS for this simulation, initial muscle activation level required to maintain the stability of a standing posture of a pedestrian in gravity field are assigned in Hill muscle card of each muscle using data reported by Kuo et al. (1993). These activation values are listed in Table A1 in appendix A. A stretch based invlountery reflex action has also been enabled in this simulation. This is to include the ability of live activated muscle to contract against a small stretch produced by an outside agency. In medical terms this kind of reflex action is known as "stretch reflex". A threshold elongation value has been defined in Hill material cards to trigger the stretch reflex in a muscle in simulation

Ackerman, (2002) has suggested a delay of 20 ms for the onset of involuntary reaction for skeletal muscles. This delay mainly represents time taken by the signal to travel through the central nervous system (CNS) circuitry. Therefore, a delay of 20 ms is assigned in Hill material card to onset the involuntary reflexive action after a muscle gets triggered for stretch reflex.

In S2, a standing pedestrian who is aware of an accident has been simulated. To model this configuration bracing in muscles has been considered. In bracing a muscle is fired at its full capacity and no signal flows from spinal cord to muscle. Therefore, to represent bracing action, all the muscles have been assigned a maximum value of 1 as an initial muscle activation level. Apart from this, reflexive action is also set off.

In S3, a standing cadaver has been simulated. This configuration has been modeled by assigning minimum value of 0.005 as an initial muscle activation level in all the muscles in A-LEMS and reflexive action has also been kept off.

Two nodes at both femur and tibia have been selected to obtain the nodal time history in simulations. Relative movements of selected nodes are then used to calculate knee bending angle and shear displacement. A transverse plane at the center of knee joint has been defined in simulations to calculate bending moment and lateral shear force. Springs of very low stiffness are modeled on each knee ligament to calculate strain time history in simulations. However, element elimination approach has also been enabled to simulate the failure in knee ligaments. Response of S1, S2 and S3 has been then compared to determine the role of muscle loading.

RESULTS AND DISCUSSION

The loading can be divided into two phases. In the initial phase, the impactor contacts the lower extremity which is initially at rest and passes energy in-elastically to the leg segments. Relative movement between tibia and femur starts only after the impactor force crosses a certain threshold, leading to fall in impactor contact force and a shear loading in the knee joint.

In the second phase, the motion of the lower extremity creates a bending motion at the knee joint called varus and valgus. The large angular displacement between femur and tibia due to this bending motion leads to stretching in ligaments and the ligament forces peak during this phase.

Below Knee Impact

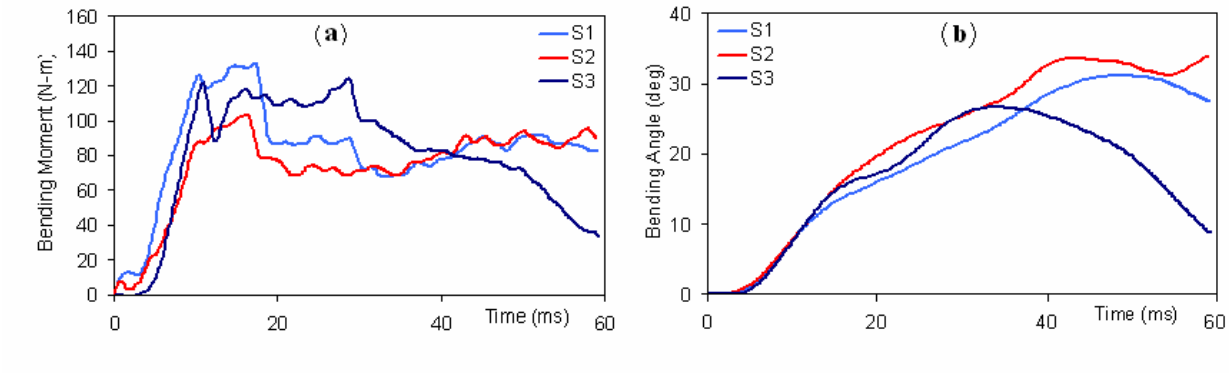

Figure 13. Comparison of (a) bending moment time history and (b) bending angle time history for three configurations (S1, S2 and S3) of a freely standing pedestrian in below-knee impact

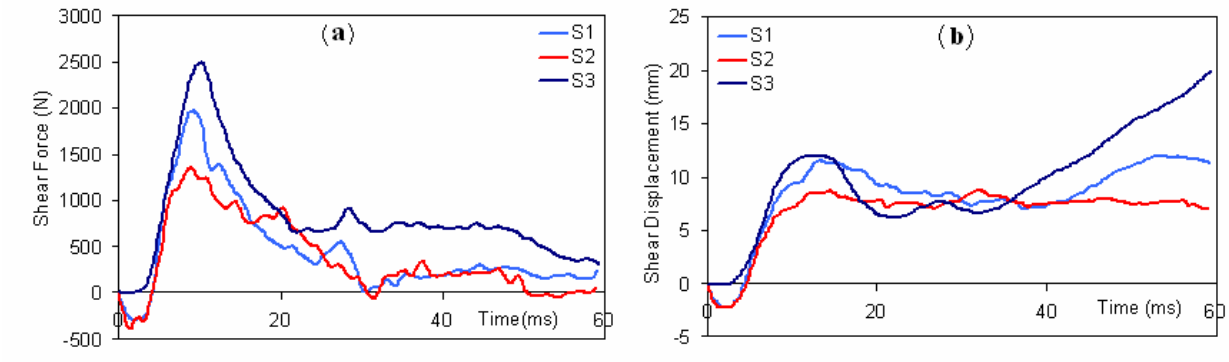

Figure 14. Comparison of (a) shear force time history and (b) shear displacement time history for three configurations (S1, S2 and S3) of a freely standing pedestrian in below-knee impact

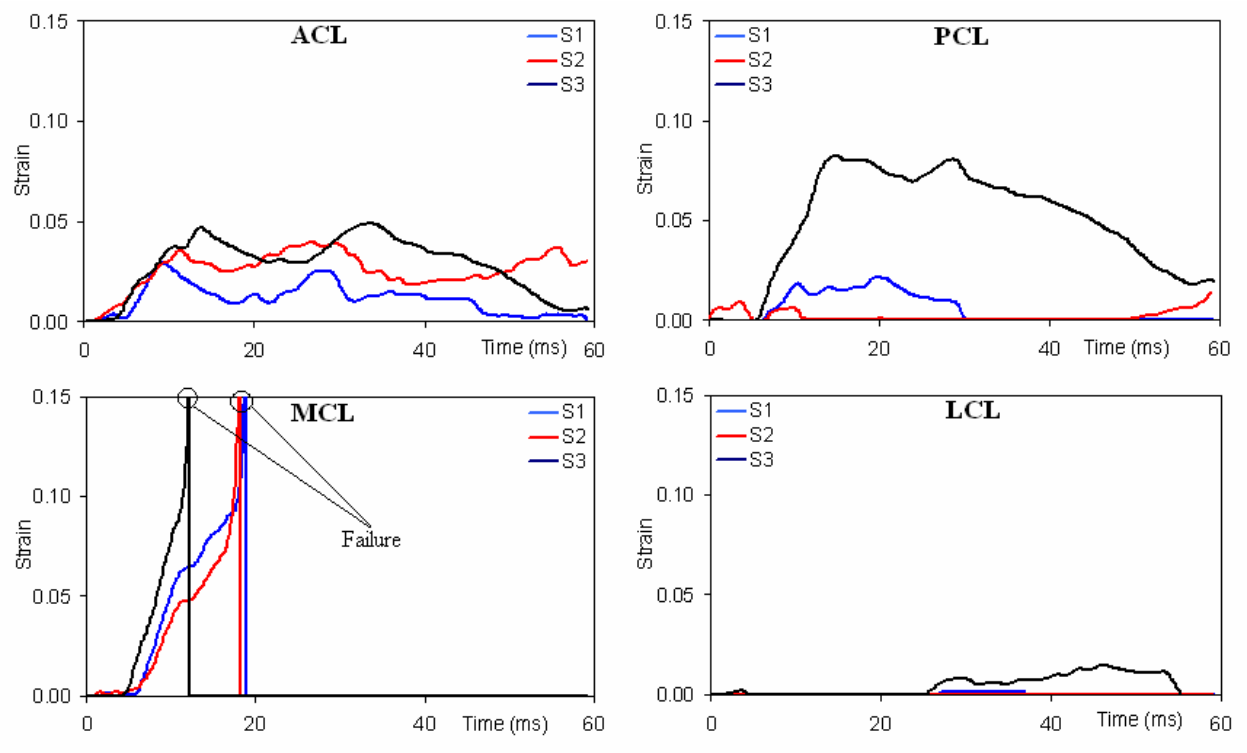

Figure 15. Comparison of strain time histroy in knee ligaments for three configurations (S1, S2 and S3) of a freely standing pedestrian in below-knee impact

Ankle Impact

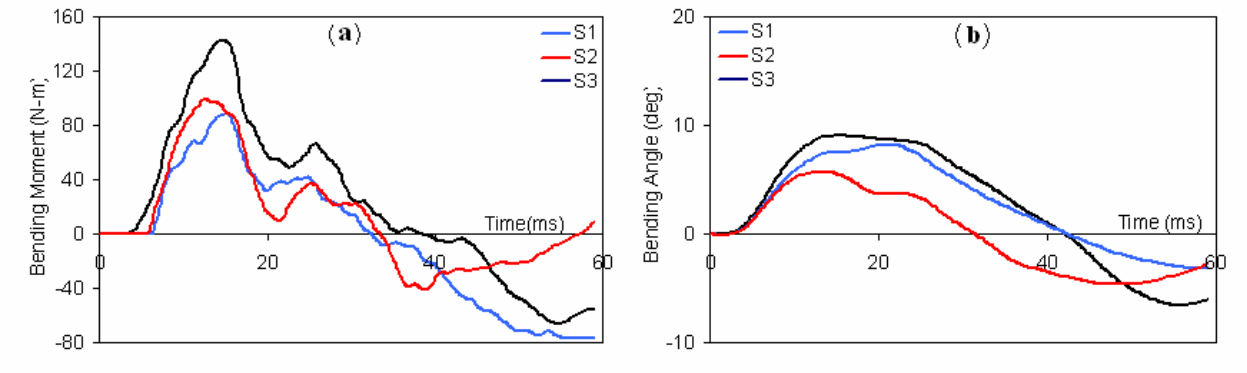

Figure 16. Comparison of (a) bending moment time history and (b) bending angle time history for three configurations (S1, S2 and S3) of a freely standing pedestrian in ankle impact

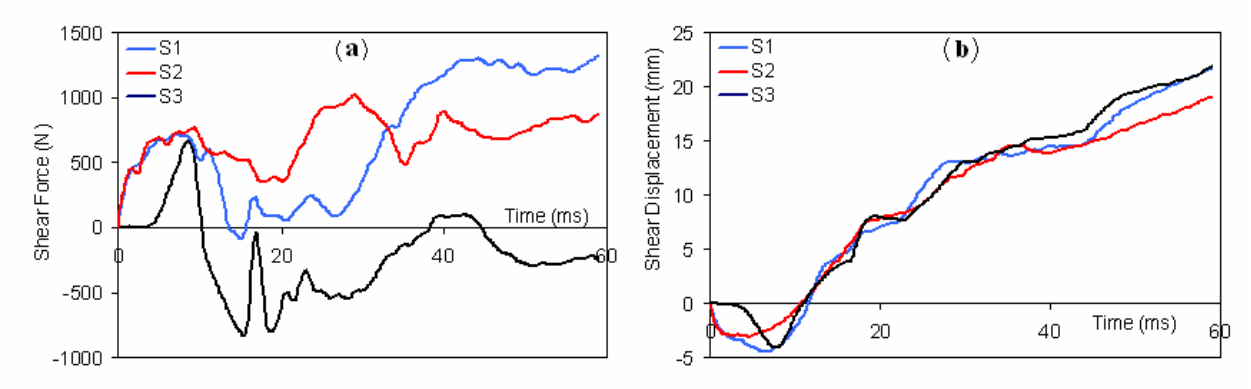

Figure 17. Comparison of (a) shear force time history and (b) shear displacement time history for three configurations (S1, S2 and S3) of a freely standing pedestrian in ankle impact

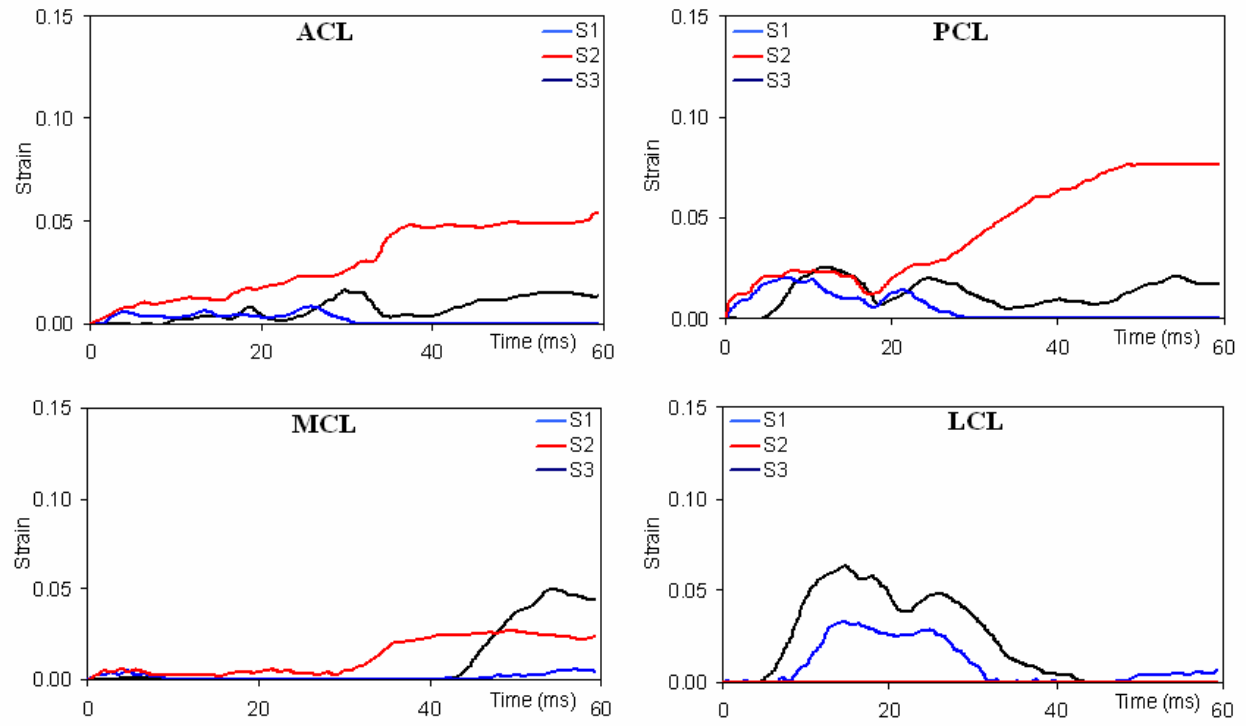

Figure 18. Comparison of strain time histroy in knee ligaments for three configurations (S1, S2 and S3) of a freely standing pedestrian in ankle impact

CONCLUSION

LIMITATIONS AND FURTHER IMPROVEMENTS

In our study, the data for point of origin and insertion was from White et al., (1989). The basis for selection of this study was the similarity in the height of the reported male specimen (177 cm) and THUMS (AM50) (175 cm), there is still a difference of 2 cm in their body height. According

to Winter et al (2005) the length of the lower extremity segment is on the average 0.53 times the total body height. Using this estimate, the difference in the lower extremity segments is about 1 cm. This difference can be further reduced by using scaling techniques. Dimensions of individual segments (femur, tibia, fibula and pelvis) required to calculate scaling factors in each direction, were not available in the literature. Apart from this, THUMS represents a 50th percentile American male and its segments length are not according to the standard fraction of total body height. However, we do not anticipate that a difference of 1 cm in length of lower extremities will change the results significantly.

In the present study we have adopted a straight line geometric model of the muscle because of the simplicity of definition using the origin and insertion locations of a muscle. This approach can lead to errors for muscles which do not work in a straight line (gracilis, semitendinosis, tibialis posterior, flexor digitorium longus, flexor hallucis longus, tibialis anterior, extensor hallucis longus, extensor digitorium longus, peroneus tertius, peroneous brevis, and peroneus longus). Multiple points could be used in the muscle definition to account for the curved path of some muscles.

For further improvements in the current finite element model, tendons should also be modeled along with the muscles to consider their effects.

Present model considers only the upper body mass; however the inclusion of its detailed geometry may affect the kinematics of knee joint.

ACKNOWLEDGEMENTS

The authors would like to acknowledge the support from the Transportation Research and Injury Prevention Program (TRIPP) at Indian Institute of Technology Delhi and the Volvo Research Foundation. The authors also acknowledge Toyota Central Research and Development Lab (TCRDL) for providing the finite element human body model, Total Human body Model for Safety (THUMS) which has been used in this study.

REFERENCES

1. Ackerman U., PDQ Physiology (2002) Ch. (2), at, www.fleshandbones.com/readingroom/pdf/226.pdf
2. Aldman, B., Kajzer, J., Bunketorp, O., Eppinger, R. (1985) An experimental study of a modified compliant bumper. In Proceedings of 10th International Technical Conference on the Experimental Safety Vehicles.
3. Ashton, S., J., Pedded, J., B., Mackay, G., M. (1977) Pedestrian injuries, the bumper and other front structure. International IRCOBI conference on the Biomechanics of Impact, pp.33-51.
4. Bhalla, K., Bose, D., Madeley, N.,J., Kerrigan, J., Crandall, J., Longhitano, D., and Takahashi, Y. (2003) Evaluation of the response of mechanical pedestrian knee joint impactors in bending and shear loading, In Proceedings of the 2003 ESV conference.
5. Bhalla, K., Takahashi, Y., Shin, J., Kam, C., Murphy, D., Drinkwater, C., J., Crandall. (2005a) Experimental investigation of the response of the human lower limb to the pedestrian impact loading environment. Society of Automotive Engineers World Congress, SAE paper, 2005-01-1877
6. Bhalla, K., Bose, D., Madeley, N. J., Kerrigan, J., Crandall, J., Longhitano D., Takahashi, Y., (2005b), Evaluation of the response of mechanical pedestrian knee joint

impactors in bending and shear loading, Proceeding of the 2005 ESV conference.

7. Bose, D., Bhalla, K., Rooij, L., Millington, S., Studley, A., and Crandall, J., (2004) Response of the knee joint to the pedestrian impact loading environment. SAE paper number 2004-01-1608.
8. Bunketorp, O. et al., (1981) Experimental studies on leg injuries in car-pedestrian impacts. IRCOBI, pp.243-255.
9. Bunketorp, O. et al., (1983) Experimental study of a compliant bumper system. SAE Paper Number 831623.
10. Butler D L, Kay M D, Stouffer D C. (1986) Comparison of material properties in fascicle bone units from human patella tendon and knee ligaments. J. Biomechanics, Vol. 19, pp. 425-432
11. Chawla, A., Mukherjee, S., Mohan, D. and Parihar, A. (2004) Validation of lower extremity model in THUMS. IRCOBI.
12. Chidester, A. B., Isenberg, R. A. (2001) Final report - the pedestrian crash data study. In Proceedings of the 17 International Technical Conference on the Enhanced Safety of Vehicles.
13. Dunmore, M., Brooks, R., McNally, D., Madeley, J., (2005). Development of an alternative frangible knee element for a pedestrian safety legform. In proceedings of 2005 IRCOBI Conference.
14. Ivarsson, J., Lessley, D., Kerrigan, J., Bhalla, K., Bose, D., Crandall, J., Kent, R., (2004) Dynamic response corridors and injury thresholds of the pedestrian lower extremities. In Proceedings of 2004 IRCOBI Conference.
15. Ivarsson, J., Kerrigan, J., Lessley, D., Drinkwater, C., Kam, C., Murphy, D., Crandall, J., Kent, R. (2005) Dynamic response of corridors of the human thigh and leg in non midpoint three-point bending. Society of Automotive Engineers World Congress, SAE paper, 2005-01-0305
16. Kajzer, J., Cavallero, S., Ghanouchi, S., Bonnoit, J., (1990) Response of the knee joint in lateral impact: Effect of shearing loads. IRCOBI.
17. Kajzer, J., Cavallero, S., Bonnoit, J., Morjane, A., Ghanouchi, S., (1993) Response of the knee joint in lateral impact: Effect of bending moment. IRCOBI.
18. Kajzer, J., Schroeder, G., Ishikawa, H., Matsui, Y., Bosch, U. (1997) Shearing and Bending Effects at the Knee Joint at High Speed Lateral Loading. Society of Automotive Engineers, SAE Paper 973326.
19. Kajzer, J., Ishikawa H., Matsui Y., Schroeder G., Bosch U. (1999) Shearing and Bending Effects at the Knee Joint at Low Speed Lateral Loading. Society of Automotive Engineers, SAE Paper 1999-01-0712.
20. Kerrigan**,** J., Bhalla, K., Madeley, N., Funk, J., Bose, D., Crandall, J. (2003) Experiments for establishing pedestrian impact lower injury criteria. SAE Paper 2003-01-0895.
21. Konosu A., Issiki, T., Tanahashi M. (2005) Development of a biofidelic flexible pedestrian leg-form impactor (Flex -PLI 2004) and evaluation of its biofedility at the component level and the assembly level. Society of Automotive Engineers World Congress, SAE paper, 2005-01-1879.
22. Kuo, A. D. and Zajac, F. E. (1993) A biomechanical analysis of muscle strength as a limiting factor in standing posture. Journal of Biomechanics 26, 137-150.
23. Maeno**,** T. and Hasegawa, J. (2001) Development of a finite element model of the total human model for safety (THUMS) and

application to car-pedestrian impacts. 17th international ESV conference, Paper No. 494.

24. Matsui, Y. (2001) Biofidelity of TRl legform impactor and injury tolerance of human leg in lateral impact. Stapp Car Crash Journal, Vol 45
25. Mizuno**,** Y. (2003) Summary of IHRA Pedestrian safety WG activities (2003) – proposed test methods to evaluate pedestrian protection afforded by passenger cars. In Proceedings of the 18th International Technical Conference on the Enhanced Safety of Vehicles.
26. Mizuno, Y. (2005) Summary of IHRA Pedestrian safety WG activities (2005) – proposed test methods to evaluate pedestrian protection afforded by passenger cars. In Proceedings of the 19th International Technical Conference on the Enhanced Safety of Vehicles.
27. Nagasaka, K., Mizuno, K., Tanaka, E., Yamamoto, S., Iwamoto, M., Miki, K. and Kajzer J. (2003) Finite element analysis of knee injury in car-to-pedestrian impacts. Traffic injury prevention, 4:345-354.
28. Ramet, M., Bouquet, R., Bermond, F., Caire, Y. (1995) Shearing and Bending Human Knee Joint Tests In Quasi-Static Lateral Load. Proceeding of the International Conference on the Biomechanics of Impact (IRCOBI).
29. Schuster, J. P., Chou, C. C., Prasad, P.,Jayaraman, G. (2000) Development and validation of a pedestrian lower limb non-linear 3-D finite element model. 2000-01-SC21, Vol. 44. Stapp Car Crash journal.
30. Soni A, Chawla A, Mukherjee S. (2006) Effect of muscle active forces on the response of knee joint at low speed lateral impacts. Society of Automotive Engineers World Congress, SAE paper, 2006-01-0460
31. Takahashi, Y., Kikuchi, Y. Konoso, A., Ishikawa, H., (2000) Development and validation of the finite element model for the human lower limb of pedestrians, Proceedings of 44th Stapp Car Crash Conference, Paper 2000-01-SC22.
32. Takahashi, Y., Kikuchi, Y. (2001) Biofidelity of test devices and validity of injury criteria for evaluating knee injuries to pedestrians, Proceedings of the ESV conference.
33. Takahashi, Y., Kikuchi, Y., Mori, F., Konosu, A. (2003) Advanced FE lower limb model for pedestrians. 18th International ESV conference, Paper no. 218.
34. White, S. C., Yack, H. J. and Winters, D. A. (1989) A three dimensional musculoskeletal model for gait analysis, anatomical variability estimates. Journal of Biomechanics 22, 885-893.
35. Wittek, A., Ishikawa, H., Matsui, Y., Konosu, A., (2000) Validation and parameter study of a multibody model for simulation of knee joint responses in lateral impacts representing car-pedestrian accidents: Influences of ligament properties and boundary conditions on model responses. Proceedings of IRCOBI conference, Montpellier, France, pp. 85-99.
36. World Bank (2001) Road Safety, http://www.worldbank.org/transport/roads/safety.html
37. Yamaguchi, G., Sawa, A., Moran, D., Fessler, M. and Winters, J. (1990) A survey of human musculotendon actuator parameters. In: Winters, J. Woo, S., (Eds.) Multiple Muscle Systems, Springer, New York pp. 717-773.

APPENDIX - A

42 lower extremity muscles are defined in the local reference frames according to White et al. (1989). Data used to define Hill muscle card for a muscle are listed in the Table A.1.

Table A.1.

Data for Lower extremity muscles

Muscle	F_{max} (N)	L_{opt} (mm)	C_{fast}	aV_{max} (Ratio of V_{max} to L_{opt})	N_a
Vastus Lateralis	1871	0.084	0.52	5.85	0.005
Vastus Intermedius	1365	0.087	0.5	5.10	0.005
Vastus Medialis	1294	0.089	0.53	5.36	0.005
Rectus Femoris	779	0.084	0.619	5.55	0.005
Soleus	2839	0.03	0.25	2.67	1*
Gastrocnemius Medialis	1113	0.045	0.518	5.74	1*
Gastrocnemius Lateralis	488	0.064	0.518	5.69	1*
Flexor Hallucis Longus	322	0.043	0.5	5.17	0.005
Flexor Digitorium Longus	310	0.034	0.5	4.58	0.005
Tibialis Posterior	1270	0.031	0.5	4.65	1*
Tibialis Anterior	603	0.098	0.27	3.28	0.5*
Extensor Digitorium Longus	341	0.102	0.527	5.31	0.005
Extensor Hallucis Longus	108	0.111	0.5	4.32	0.005
Peroneus Brevis	348	0.05	0.375	4.59	1*
Peroneus longus	754	0.049	0.375	4.35	0.005
Peroneus Tertius	90	0.079	0.375	4.76	0.005
Biceps Femoris (LH)	717	0.109	0.331	3.55	1*
Biceps Femoris (SH)	402	0.173	0.331	3.91	1*
Semimembranosus	1030	0.08	0.5	5.61	1*
Semitendinosus	328	0.201	0.5	4.76	1*
Piriformis	296	0.026	0.5	5.71	0.005
Pectineus	177	0.133	0.5	4.62	0.005
Obturatorius Internus	254		0.5	5.71	0.005
Obturatorius Externus	109		0.5	5.71	0.005
Gracilis	108	0.352	0.5	5.13	0.005
Adductor Brevis 1	286	0.133	0.5	5.17	0.005
Adductor brevis 2	286	0.133	0.5	5.22	0.005
Adductor Longus	418	0.138	0.5	4.69	0.5*
Adductor Mangus 1	346	0.087	0.416	5.07	0.005
Adductor Mangus 2	444	0.121	0.416	5.07	0.005
Adductor Mangus 3	155	0.131	0.416	5.07	0.005
Glutaeus Maximus 1	382	0.142	0.476	5.53	0.005
Glutaeus Maximus 2	546	0.147	0.476	5.53	0.005
Glutaeus Maximus 3	368	0.144	0.476	5.53	0.005
Glutaeus Medius 1	546	0.054	0.5	5.71	0.005
Glutaeus Medius 2	382	0.084	0.5	5.71	0.005
Glutaeus Medius 3	435	0.065	0.5	5.71	0.005
Glutaeus Minimus 1	180	0.068	0.5	5.71	0.005

Glutaeus Minimus 2	190	0.056	0.5	5.71	0.005
Glutaeus Minimus 3	215	0.038	0.5	5.71	0.005
Sartorius	104	0.579	0.504	5.03	0.005
Tensor Fasciae Latae	155	0.095	0.5	5.71	1*

* - Na represents initial activation level in a muscle during standing posture. These values have been taken from Kuo et al., (1993).